

SUPPLEMENTARY INFORMATION

CATESTATIN GLY364SER VARIANT ALTERS SYSTEMIC BLOOD PRESSURE AND THE RISK FOR HYPERTENSION IN HUMAN POPULATIONS VIA ENDOTHELIAL NO PATHWAY

Malapaka Kiranmayi¹, Venkat R Chirasani¹, Prasanna K R Allu^{1,7}, Lakshmi Subramanian¹, Elizabeth E Martelli², Bhavani S Sahu^{1,8}, Durairajpandian Vishnuprabu³, Rathnakumar Kumaragurubaran¹, Saurabh Sharma⁴, Dhanasekaran Bodhini⁵, Madhulika Dixit¹, Arasambattu K Munirajan³, Madhu Khullar⁴, Venkatesan Radha⁵, Viswanathan Mohan⁵, Ajit S Mulasari⁶, Sathyamangla V Naga Prasad², Sanjib Senapati¹, Nitish R Mahapatra^{1,*}

from the

¹Department of Biotechnology, Bhupat and Jyoti Mehta School of Biosciences, Indian Institute of Technology Madras, Chennai, Tamil Nadu, India

²Department of Molecular Cardiology, Lerner Research Institute, Cleveland Clinic, Ohio, USA

³Department of Genetics, University of Madras, Chennai, Tamil Nadu, India

⁴Department of Experimental Medicine and Biotechnology, Postgraduate Institute of Medical Education and Research, Chandigarh, India

⁵Department of Molecular Genetics, Madras Diabetes Research Foundation, Chennai, Tamil Nadu, India

⁶Institute of Cardiovascular Diseases, Madras Medical Mission, Chennai, Tamil Nadu, India

⁷Department of Medicine, University of California San Francisco, California, USA

⁸Department of Clinical Biochemistry, University of Cambridge, Cambridge, UK

DETAILED METHODS

Human subjects and study design for primary study (Chennai population)

The present case-control study enrolled a total of 3200 unrelated human subjects, comprising 1705 hypertensive/diabetic cases (with no history of cancer/kidney disease), 519 coronary artery disease (CAD) samples and 976 controls (with no history of hypertension/diabetes/cancer/kidney disease). The subjects were recruited from the urban cosmopolitan population of Chennai, the fourth largest city in India, at three independent centres - hypertensive/diabetic cases from The Institute of Cardiovascular Diseases, Madras Medical Mission (MMM) and Madras Diabetes Research Foundation (MDRF) and CAD samples from Madras Medical College (MMC). At MMM, peripheral venipuncture was carried out to collect blood samples. These samples were stored in EDTA-containing tubes for the isolation of genomic DNA at a later time. Plasma samples were also collected, aliquoted, and stored at -80°C for assaying various biochemical parameters. At MDRF, the samples were collected in the form of genomic DNA. At MMC, the samples were collected in the form of genomic DNA. Each subject gave informed, written consent for the use of their sample in this study. The study was approved by the Institute Ethics Committees at MMM, MDRF, MMC and Indian Institute of Technology Madras. Data was also collected regarding the demographic parameters (age, sex), physical parameters (height, weight, and body mass index [BMI]), physiological parameters (systolic blood pressure (SBP), diastolic blood pressure (DBP), mean arterial pressure (MAP), heart rate (HR), left ventricular dimension at end of systole (LVIDs) and left ventricular dimension at end of diastole (LVIDd)), biochemical parameters (hemoglobin, sodium, potassium, urea, creatinine, blood sugar, total cholesterol [TC], triglycerides [TGL], insulin, HOMA-IR index and HbA1c) and medical history (current medication, family history of cardiovascular and renal disease states) of the cases and

controls. Blood pressure was measured on the sitting position by experienced nursing staff using a brachial oscillometric cuff, and triplicate values were averaged. Supplementary Table S2 describes the demographic, physiological and biochemical parameters of the study subjects by case, control status. In the Chennai DM/HTN/controls population, the average age of the subjects was ~43 years. Out of the 1705 cases, 721 were essential hypertensives, 472 were diabetic and 512 had both hypertension and diabetes. 74% of the hypertensive subjects were on antihypertensive medications such as angiotensin II receptor blocker, angiotensin convertase enzyme inhibitors, beta blockers and calcium channel blockers. In case of diabetic subjects, 29% were receiving diabetic medications such as oral hypoglycemic agents and insulin. The diabetic/hypertensive cases differed from the controls in terms of BMI ($p<0.001$), SBP ($p<0.001$), DBP ($p<0.001$), MAP ($p<0.001$), LVIDs ($p=0.001$), blood sugar ($p<0.001$), TC ($p<0.001$), TGL ($p<0.001$) and fasting blood sugar (FBS) insulin ($p<0.001$). The CAD cases had an average age of 51 years.

Human subjects and study design for replication population (Chandigarh)

To validate our primary study in a geographically separated population, we studied 760 unrelated human subjects from North India (Chandigarh). The human subjects were recruited at the Post Graduate Institute of Medical Education and Research (PGIMER), Chandigarh, and consisted of 401 hypertensive cases (with no history of cancer/kidney disease) and 359 normotensive controls (with no history of hypertension/diabetes/cancer/kidney disease). Supplementary Table S3 describes the demographic, physiological and biochemical parameters of the study subjects by case, control status. The samples were obtained in the form of genomic DNA for all the 760 human subjects. All subjects were informed of the purpose of the study and their written consent was obtained. The study was approved by the Institute Ethics Committee at PGIMER. Data regarding the demographic parameters (age, sex), physical parameters (BMI), physiological

parameters (pre-treatment SBP, DBP, and MAP), biochemical parameters (hemoglobin, sodium, potassium, urea, creatinine, blood sugar, TC, TGL) and current medication of the subjects was collected. In the Chandigarh population, the average age of the subjects was ~53 years. The hypertensive cases differed from the controls in terms of SBP ($p < 0.001$), DBP ($p < 0.001$) and MAP ($p < 0.001$).

Genotyping of the CST 364Ser variant

Sanger's sequencing: Out of the 3960 samples, 1763 samples were genotyped using the PCR-purification-Sanger's sequencing protocol as described previously ¹. Genomic DNA was prepared from the EDTA-anti-coagulated blood samples according to the manufacturer's instructions using the FlexiGene DNA kit (Qiagen, USA). With this genomic DNA as template, forward primer: 5'-GAGTGGCAGAGACTGGGAAAATG-3' and reverse primer: 5'-ACAGAGCTGGCTCCCGCCC-3' were used to PCR amplify the exon-7 region of *CHGA*. The PCR amplicons were purified using QIAquick PCR purification columns (Qiagen, USA) and sequenced using an Applied Biosystems 3130 Genetic Analyzer (USA). All the samples were sequenced initially using the forward primer (as described above). Each chromatogram was manually checked for the confirmation of the genetic variants. In case of any ambiguity regarding a polymorphism, the sample was re-sequenced using the reverse primer (as described above).

Taqman® assay: The remaining 2197 samples were genotyped using the Taqman® assay. Taqman® SNP genotyping assay was performed in a 384 well microAmp PCR plate (Applied Biosystems [ABI], USA). The 5 µl PCR comprised of 10 ng genomic DNA and 2.5 µl of 2X TaqMan® Universal PCR master mix No UNG and 0.125 µl of 40X TaqMan® SNP Genotyping assay mix (Probes and Primers) (ABI, USA). Absolute Quantification was performed according to the manufacturer's recommendation (2 min at 50°C, 10 min at 95°C followed by 15 sec at

92°C and 60 sec at 60°C for 40 cycles) and Allelic discrimination with endpoint detection of fluorescence was performed in ABI 7900HT real-time PCR system (ABI, USA). Non-template controls and positive controls (known homozygous variants) were routinely added in each reaction. Genotype calls were selected by 95% quality calls using Sequence Detection Software (SDS) (ABI, USA).

Estimation of biochemical parameters

Standard biochemical assays were used to measure biochemical parameters such as glucose (random blood sugar, fasting blood sugar, and post-glucose blood sugar), total cholesterol, triglycerides, urea, creatinine, hemoglobin, sodium and potassium levels in the plasma. The blood pressure readings are an average of triplicate values recorded in the sitting position using a brachial oscillometric cuff by experienced nursing staff.

Data representation and statistical analysis

The experimental data results and the human study phenotypic parameters are expressed as mean \pm SE. Allele frequencies were estimated by gene counting. A Pearson's χ^2 test was employed to compare the distribution of the genotypes. Statistical analysis was carried out using the Statistical Package for Social Sciences (SPSS) Version 21.0. To identify the risk of the genotype for any of the disease conditions, logistic regression analysis was carried out using the disease condition (DM, HTN, CAD, metabolic disease) as the dependent variable and the genotypes (risk factors) and age, sex and BMI (covariates adjusted in the analysis) as the independent variables. Outliers with abnormal values for any of the parameters were removed by quartile analysis. To evaluate the association of the variant allele with the phenotypic parameters, the Levene's test for equality of variance and t-test for equality of means were performed with the homozygotes for the major allele (wild-type CST-364Gly/Gly) individuals coded as 0 and the heterozygotes as well as homozygotes for the minor allele (CST-364Gly/Ser and CST-364Ser/Ser, respectively) coded as

1. Owing to their small numbers (n=18) in the overall population, the homozygous variant individuals were grouped with the heterozygous variant individuals. The overall population was further divided into different disease groups (all cases, only hypertensives, only diabetics, subjects with both hypertension and diabetes, CAD, controls) and statistical analysis was carried out among these groups as well to identify any allele-specific associations with the various disease conditions. Analysis of covariance (ANCOVA) was also carried out in a univariate general linear model after adjusting for age as a covariate. Haploview 4.2 was used for linkage disequilibrium analysis. Deviations from the Hardy-Weinberg equilibrium were calculated using the online calculator provided by Tufts University, Boston, MA: <http://www.tufts.edu/mcourt01/Documents/Court%20lab%20-%20HW%20calculator.xls>. A p value of <0.05 was chosen as statistically significant. The power of the study was calculated using Quanto version 1.2.4. Meta-analysis was carried out using the OpenMeta[Analyst] software (www.cebm.brown.edu/open_meta/).

Synthesis of CST peptides

The CST wild type (CST-WT, SSMKLSFRARAYGFRGPGPQL) and CST-364Ser variant (CST-Ser364, SSMKLSFRARAYSFRGPGPQL) peptides were synthesized by solid phase method and purified to 95% homogeneity as described previously ¹. The purity and molecular weights of these peptides were verified by analytical high performance liquid chromatography and mass spectrometry.

Human umbilical vein endothelial cells (HUVECs) isolation and culture conditions

Experimental procedures involving umbilical cords were reviewed and approved by the IIT Madras institutional ethics committee in accordance with Declaration of Helsinki revised in 2000 (reference number: IITM IEC No. 2009024). HUVECs were isolated from umbilical cords by

digestion with collagenase as described previously². HUVECs in passage 2 were used for all the experiments. Cells were cultured in MCDB131 medium (from HiMedia) supplemented with EGM™ SingleQuots™ (Lonza, USA). Isolated cells were seeded onto fibronectin coated T-25 flasks and grown to confluence with 10% Fetal Bovine Serum (FBS). Cells were sub-cultured for experimental conditions either in 6-well or 24 well fibronectin-coated tissue culture dishes.

Measurement of nitric oxide (NO) levels in cultured HUVECs

NO levels in HUVECs were measured by 4, 5-Diaminofluorescein diacetate (DAF-2 DA) method as described previously³. HUVECs were first seeded in 24-well plates and on reaching 60-70% confluence (i.e., 24 hours after seeding), cells were serum-starved for 12 hours and then treated with different doses of CST-WT or CST-364Ser for 20 min at 37°C. The peptides were prepared in serum-free media. After the 20 minute treatment, serum-free media containing the peptides was removed and the cells were incubated with 10 µmol/L DAF-2 DA (Sigma-Aldrich) and 1.0 mmol/L L-Arginine (nitric oxide synthases [NOS] substrate; Sigma-Aldrich) in serum-free media for 20 min at 37°C. The cells were then washed twice with phosphate buffer saline (PBS) and the fluorescence was detected by a Nikon-Ti Eclipse fluorescence microscope (Japan) with excitation wavelength of 485 nm and emission wavelength of 530 nm. For each condition, three fields were captured. The NO index was arrived at by measuring the mean fluorescence intensity for n=50 cells/field using ImageJ software. The experiments were repeated at least 3 times. For the antagonists experiments, the cells were treated with 300 nmol/L CGP 20712 and 100 nmol/L ICI 118551 for 20 min at 37°C before treatment with the peptides. The antagonists were prepared in serum-free media.

ADRB1/2 HEK-293 cells culture and treatment

Human embryonic kidney (HEK) 293 cells that stably over-express ADRB1/2 (ADRB1/2 HEK-293) were used to test whether CST peptides bind to ADRB1/2. ADRB1/2 HEK-293 cells were maintained in minimal essential medium (MEM) supplemented with 10% FBS and penicillin-streptomycin at 37°C. Cells were seeded at a density of $\sim 1 \times 10^6$ cells/100 mm and were subjected to treatments at 60-80% confluence. At 60-80% confluence cells were serum starved in MEM at 37°C for 4 hours. To test whether CST treatment alters ADRB1/2 agonist responses, ADRB1/2 HEK-293 cells were pre-incubated with CST-WT and CST-364Ser peptides (10 $\mu\text{mol/L}$) for 45 minutes followed by ADRB agonist isoproterenol (10 $\mu\text{mol/L}$) for 0, 5 and 10 minutes.

Isolation of ADRB1/2-expressing plasma membranes

Purification of plasma membrane was performed as described previously^{4,5}. Plasma membranes from control HEK-293 and ADRB1/2 HEK-293 cells were isolated by briefly homogenizing cells in ice-cold lysis buffer containing 5 mmol/L Tris-HCl (pH 7.5), 5 mmol/L EDTA, 1 mmol/L PMSF, and 2 $\mu\text{g/ml}$ Leupeptin and Aprotinin. Cell debris/nuclei were removed by centrifugation at 1000 x g for 5 minutes at 4°C. Supernatant was transferred to a new tube and subjected to centrifugation at 37,000 x g for 30 minutes at 4°C. The pellet containing plasma membrane was re-suspended in 75 mmol/L Tris-HCl (pH 7.5), 2 mmol/L EDTA, 12.5 mmol/L MgCl_2 and was used for ligand binding assays.

Radio-ligand binding and competition binding assays

To test for the level of ADRB1/2 expression in ADRB1/2 HEK-293 cells, [¹²⁵I]-cyanopindolol saturation radio-ligand binding was performed on the plasma membranes isolated from control HEK-293 and ADRB1/2 HEK-293 cells as described previously^{4,5}. Briefly, 20 μg of plasma membranes were incubated with saturating concentrations of cyanopindolol (250 pmol/L) alone

or along with 100 $\mu\text{mol/L}$ Propranolol. Propranolol was used for determining non-specific binding. The samples were incubated at 37°C for 1 hour, harvested using BRANDEL cell harvester system (BRANDEL, USA) on to a GF/C filter paper and the bound ligand ascertained using BECKMAN LS6000IC (BECKMAN, USA) gamma counter.

An indirect, competitive ligand binding assay was performed where the binding of CST peptides, CST-WT and CST-364Ser, to the ADRB1/2 over-expressing membrane surface in ADRB1/2-HEK-293 cells was measured in terms of their ability to displace the bound high-affinity radio-labeled ligand, cyanopindolol. 20 μg of plasma membranes were incubated with saturating concentrations of cyanopindolol and increasing concentrations of the CST peptides (from 10 pmol/L to 1 mmol/L). Following incubation at 37°C for 1 hour, samples were harvested using BRANDEL cell harvester system (BRANDEL, USA) and the bound ligand was determined using the BECKMAN LS6000IC (BECKMAN, USA) gamma counter.

Western immunoblotting

Activation of ADRB1/2 in HEK-293 cells was assessed in terms of activation of extracellular regulated kinase (ERK) by performing immunoblotting and detection of phospho-ERK as described previously⁶. Cells were harvested in NP40 lysis buffer containing 20 mmol/L Tris (pH 7.4), 137 mmol/L NaCl, 1% NP-40, 1 mmol/L PMSF, 20% Glycerol, 10 mmol/L NaF, 1 mmol/L Sodium Orthovanadate, 2 $\mu\text{g/ml}$ Leupeptin and Aprotinin. The lysates were cleared by centrifugation at 12000 x g for 15 min at 4°C. 70-120 μg of the supernatant cell lysate was resolved by SDS-PAGE and transferred onto PVDF membranes (BIO-RAD) for western immunoblotting analysis. The membranes were blocked with 5% BSA and incubated with anti-phospho ERK antibody at 1:1000 dilution to recognize activated ERK. Following primary antibody incubation, appropriate secondary antibody (1:3000) was used and detection was

carried out using enhanced chemiluminescence. Quantitative densitometric analysis was carried out using the NIH Image J software.

Activation of eNOS in HUVECs with/without treatment with CST peptides was assessed by western blotting and detection of Ser¹¹⁷⁷ phosphorylated eNOS. HUVECs were first seeded in 12-well plates and on reaching 60-70% confluence (i.e., 24 hours after seeding), cells were serum-starved for 12 hours and then treated with 1 nmol/L CST-WT or CST-364Ser for 20 min at 37°C. Cells were harvested in RIPA lysis buffer containing 50 mmol/L Tris (pH 8.0), 150 mmol/L NaCl, 1% Triton X-100, 1x Protease Inhibitor Cocktail, 0.1% SDS. The lysates were cleared by centrifugation at 12000 x g for 15 min at 4°C. 30-40 µg of the supernatant cell lysate was resolved by SDS-PAGE and transferred onto PVDF membrane (BIO-RAD) for western immunoblotting analysis. The membrane was blocked with 5% BSA for Ser¹¹⁷⁷ and 3% BSA for total eNOS at room temperature for an hour. The membrane was then incubated with anti-phospho Ser¹¹⁷⁷ eNOS antibody (Cell Signaling, USA) and anti-total eNOS antibody (Santa Cruz, USA) at 1:1000 dilutions to recognize phospo-eNOS and total eNOS. Following primary antibody incubation, appropriate secondary antibody (1:5000) was used and detection was carried out using enhanced chemiluminescence. Quantitative densitometric analysis was carried out using the NIH Image J software.

Modelling of the ADRB1 and ADRB2 receptors and the CST-WT and CST-364Ser peptide structures

The crystal structure of ADRB2 with resolution 2.4 Å was obtained from protein data bank (PDB ID:2RH1) ⁷. The bound ligands and crystal water were stripped out from the protein structure and subsequently energy minimized to obtain a more sophisticated model of ADRB2 for protein-protein docking. The structure of ADRB1 was modelled based on the structure of ADRB2 as a

template. The regions in ADRB1 with poor structural homology were excluded from the structure during refinement.

The structure of 21-mer human wild-type CST (CST-WT) has already been determined by NMR (PDB ID:1LV4)⁸. However, the absence of any secondary structural elements in the NMR structure called for a more detailed elucidation of the peptide's conformation. In this work, we generated 3D structures of CST-WT and its variant CST-364Ser following a similar protocol as proposed earlier⁹. The NMR structure of CST was downloaded from protein data bank and subjected to short energy minimization for optimal positioning of the side chains. Residue Gly364 in the CST structure was mutated to 364Ser using Modeller 9v13¹⁰ and a short energy minimization was imposed to optimize the side chain positions. The final refinements for CST-WT as well as CST-364Ser were carried out by molecular dynamics (MD) simulations. The minimized structures were subsequently subjected to 300 nanoseconds explicit water MD simulations to generate an ensemble of both CST-WT and CST-364Ser conformations.

MD simulations methodology

All the simulations were performed using Gromacs-4.5.5 simulation package¹¹ and AMBER99SB force-field parameters¹². First, the system was energy minimized using conjugate gradient and steepest descent algorithms, each with 1000 steps. The energy-minimized protein structure was subsequently solvated in a cubic periodic box with about 2400 explicit water molecules. In MD simulations, an initial drift is anticipated as the peptide residues diminish any unfavorable interactions and the solvent molecules relax around them. Hence, the structural analyses of the peptides were executed on the last 25 ns simulation data. TIP3P model was used to describe the water molecules. A salt concentration of 0.15 M was maintained with appropriate number of Na⁺ and Cl⁻ ions to mimic the physiological ionic strength. The solvated system was again energy minimized and subsequently heated to 310 K. The system was equilibrated in NPT

ensemble at 1 atm and 310 K for about 10 ns, by when the solvent density, system temperature reached a plateau. This followed a production phase of 300 ns, on which all analyses were performed. Long-range electrostatic interactions were described using Particle Mesh Ewald sum technique¹³ with a real space cut-off of 1.0 nm and SHAKE algorithm¹⁴ was used to constrain all bonds involving hydrogen atoms.

Protein-protein docking of CST-WT and CST-364Ser with ADRB1/2 receptors

Protein-protein docking of CST peptides on ADRB1/2 was performed using ZDOCK docking algorithm¹⁵ to locate the probable binding sites of CST peptides in ADRB1/2 structure. ZDOCK performs efficient global docking search on a 3D grid by using Fast Fourier Transform algorithm and scores docked complexes based on combination of shape complementarity, electrostatics and statistical potential terms¹⁶. During molecular docking, CST peptides were allowed to search the extra cellular region of the ADRB1/2 receptors to identify the best binding location. ZDOCK predicted 100 binding modes of CST peptides with ADRB1/2, which were ranked according to ZDOCK docking score. The best docked complex was then identified based on this score.

All the structural figures were rendered using Visual Molecular Dynamics (VMD)¹⁷. The ADRB2-CST interactions were identified using PDBsum¹⁸ and cyanopindolol-ADRB2 interactions were identified using LigPlot+¹⁹.

REFERENCES FOR SUPPLEMENTARY INFORMATION

1. Sahu BS, Obbineni JM, Sahu G, Allu PK, Subramanian L, Sonawane PJ, Singh PK, Sasi BK, Senapati S, Maji SK, Bera AK, Gomathi BS, Mullasari AS, Mahapatra NR. Functional genetic variants of the catecholamine-release-inhibitory peptide catestatin in an indian population: Allele-specific effects on metabolic traits. *J Biol Chem.* 2012;287:43840-43852.
2. Giri H, Muthuramu I, Dhar M, Rathnakumar K, Ram U, Dixit M. Protein tyrosine phosphatase shp2 mediates chronic insulin-induced endothelial inflammation. *Arterioscler Thromb Vasc Biol.* 2012;32:1943-1950.
3. Kesavan R, Potunuru UR, Nastasijevic B, T A, Joksic G, Dixit M. Inhibition of vascular smooth muscle cell proliferation by gentiana lutea root extracts. *PLoS One.* 2013;8:e61393.
4. Naga Prasad SV, Barak LS, Rapacciuolo A, Caron MG, Rockman HA. Agonist-dependent recruitment of phosphoinositide 3-kinase to the membrane by beta-adrenergic receptor kinase 1. A role in receptor sequestration. *J Biol Chem.* 2001;276:18953-18959.
5. Vasudevan NT, Mohan ML, Gupta MK, Hussain AK, Naga Prasad SV. Inhibition of protein phosphatase 2a activity by pi3kgamma regulates beta-adrenergic receptor function. *Mol Cell.* 2011;41:636-648.
6. Noma T, Lemaire A, Naga Prasad SV, Barki-Harrington L, Tilley DG, Chen J, Le Corvoisier P, Violin JD, Wei H, Lefkowitz RJ, Rockman HA. Beta-arrestin-mediated beta1-adrenergic receptor transactivation of the egfr confers cardioprotection. *J Clin Invest.* 2007;117:2445-2458.
7. Cherezov V, Rosenbaum DM, Hanson MA, Rasmussen SG, Thian FS, Kobilka TS, Choi HJ, Kuhn P, Weis WI, Kobilka BK, Stevens RC. High-resolution crystal structure of an

- engineered human beta2-adrenergic g protein-coupled receptor. *Science*. 2007;318:1258-1265.
8. Preece NE, Nguyen M, Mahata M, Mahata SK, Mahapatra NR, Tsigelny I, O'Connor DT. Conformational preferences and activities of peptides from the catecholamine release-inhibitory (catestatin) region of chromogranin a. *Regul Pept*. 2004;118:75-87.
 9. Allu PK, Chirasani VR, Ghosh D, Mani A, Bera AK, Maji SK, Senapati S, Mullasari AS, Mahapatra NR. Naturally occurring variants of the dysglycemic peptide pancreastatin: Differential potencies for multiple cellular functions and structure-function correlation. *J Biol Chem*. 2014;289:4455-4469.
 10. Webb B, Sali A. Comparative protein structure modeling using modeller. *Curr Protoc Bioinformatics*. 2014;47:1-5.
 11. Hess B, Kutzner C, van der Spoel D, Lindahl E. Gromacs 4: Algorithms for highly efficient, load-balanced, and scalable molecular simulation. *Journal of Chemical Theory and Computation*. 2008;4:435-447.
 12. Hornak V, Abel R, Okur A, Strockbine B, Roitberg A, Simmerling C. Comparison of multiple amber force fields and development of improved protein backbone parameters. *Proteins*. 2006;65:712-725.
 13. Essmann U, Perera L, Berkowitz ML, Darden T, Lee H, Pedersen LG. A smooth particle mesh ewald method. *The Journal of Chemical Physics*. 1995;103:8577-8593.
 14. Ryckaert J-P, Ciccotti G, Berendsen HJC. Numerical integration of the cartesian equations of motion of a system with constraints: Molecular dynamics of n-alkanes. *Journal of Computational Physics*. 1977;23:327-341.
 15. Pierce BG, Wiehe K, Hwang H, Kim BH, Vreven T, Weng Z. Zdock server: Interactive docking prediction of protein-protein complexes and symmetric multimers. *Bioinformatics*. 2014;30:1771-1773.

16. Mintseris J, Pierce B, Wiehe K, Anderson R, Chen R, Weng Z. Integrating statistical pair potentials into protein complex prediction. *Proteins*. 2007;69:511-520.
17. Humphrey W, Dalke A, Schulten K. Vmd: Visual molecular dynamics. *J Mol Graph*. 1996;14:33-38.
18. de Beer TA, Berka K, Thornton JM, Laskowski RA. Pdbsum additions. *Nucleic Acids Res*. 2014;42:D292-D296.
19. Laskowski RA, Swindells MB. Ligplot+: Multiple ligand-protein interaction diagrams for drug discovery. *J Chem Inf Model*. 2011;51:2778-2786.
20. Wen G, Mahata SK, Cadman P, Mahata M, Ghosh S, Mahapatra NR, Rao F, Stridsberg M, Smith DW, Mahboubi P, Schork NJ, O'Connor DT, Hamilton BA. Both rare and common polymorphisms contribute functional variation at chga, a regulator of catecholamine physiology. *Am J Hum Genet*. 2004;74:197-207.
21. Choi Y, Miura M, Nakata Y et al. A common genetic variant of the chromogranin a-derived peptide catestatin is associated with atherogenesis and hypertension in a japanese population. *Endocr J*. 2015;62:797-804.
22. Biesecker LG, Mullikin JC, Facio FM et al. The clinseq project: Piloting large-scale genome sequencing for research in genomic medicine. *Genome Res*. 2009;19:1665-1674.

SUPPLEMENTARY TABLES

Supplementary Table S1: Genetic variants identified in the CST domain of *CHGA* in various world populations. *

SNP	rs number	Wild-type base	Variant base	Reference
Y363Y	rs9658666	C	T	Wen <i>et. al.</i> 2004 ²⁰
G364S	rs9658667	G	A	Wen <i>et. al.</i> 2004 ²⁰ , Sahu <i>et. al.</i> 2012 ¹
G367V	rs200576557	G	T	Sahu <i>et. al.</i> 2012 ¹
P370L	rs9658668	C	T	Wen <i>et. al.</i> 2004 ²⁰
R374Q	rs9658669	G	A	Wen <i>et. al.</i> 2004 ²⁰

* The naturally-occurring genetic variants discovered in the CST domain of *CHGA* in different world populations are listed along with their rs numbers and the change in nucleotide.

Supplementary Table S2: Clinical characteristics of controls and cases in South Indian populations.*

Parameter	Controls		DM, HTN cases		p value	CAD cases		p value
	N	Mean \pm SE	N	Mean \pm SE		N	Mean \pm SE	
Age (years)	976	39.24 \pm 0.348	1702	45.97 \pm 0.256	<0.001	514	50.95 \pm 0.483	<0.001
Sex (M/F)	976	51.8%/48.2%	1705	58.5%/41.5%		518	87.3%/12.7%	
Height (cm)	600	163.18 \pm 0.318	906	162.96 \pm 0.281	0.271	338	161.61 \pm 0.389	<0.001
Weight (kg)	600	64.59 \pm 0.375	902	65.34 \pm 0.294	0.488	349	63.05 \pm 0.540	0.020
Body Mass Index (kg/m ²)	976	23.75 \pm 0.118	1700	24.81 \pm 0.091	<0.001		NA	
Heart Rate (beats/minute)	600	77.24 \pm 0.334	901	77.19 \pm 0.263	1.000	495	79.92 \pm 0.570	<0.001
Systolic Blood Pressure (mm Hg)	868	120.03 \pm 0.439	1208	142.83 \pm 0.545	<0.001	505	127.45 \pm 0.887	<0.001
Diastolic Blood Pressure (mm Hg)	868	74.58 \pm 0.278	1208	85.66 \pm 0.334	<0.001	505	82.15 \pm 0.530	<0.001
Mean Arterial Pressure (mm Hg)	868	89.70 \pm 0.290	1208	104.77 \pm 0.367	<0.001	505	97.26 \pm 0.599	<0.001
LVIDd (mm)	600	44.37 \pm 0.121	906	44.86 \pm 0.117	0.052		NA	
LVIDs (mm)	600	26.73 \pm 0.123	906	27.40 \pm 0.115	0.001		NA	
Haemoglobin (g/dl)	616	13.36 \pm 0.190	1095	13.51 \pm 0.114	0.947		NA	
Sodium (meq/l)	562	139.24 \pm 0.129	906	136.90 \pm 0.172	<0.001	336	135.36 \pm 0.516	<0.001
Potassium (meq/l)	562	4.08 \pm 0.070	906	4.06 \pm 0.044	1.000	339	3.79 \pm 0.104	0.028
Urea (mg/dl)	668	20.86 \pm 0.269	1397	24.38 \pm 0.244	<0.001		NA	
Creatinine (mg/dl)	668	0.81 \pm 0.007	1397	0.88 \pm 0.005	<0.001		NA	

Random Blood Sugar (mg/dl)	562	96.03 ± 0.687	905	107.78 ± 1.376	<0.001	358	131.85 ± 3.363	<0.001
Total Cholesterol (mg/dl)	937	173.17 ± 1.095	1690	183.77 ± 1.044	<0.001	109	176.28 ± 3.753	0.381
Triglycerides (mg/dl)	937	117.85 ± 1.887	1689	159.22 ± 2.464	<0.001	112	137.92 ± 5.333	<0.001
High Density Lipoproteins (mg/dl)	937	40.41 ± 0.368	1691	40.48 ± 0.268	1.000	76	39.3 ± 0.714	0.297
Low Density Lipoproteins (mg/dl)	937	106.54 ± 0.922	1691	112.61 ± 0.842	<0.001	11	133.45 ± 9.802	0.001
Very Low Density Lipoproteins (mg/dl)	376	23.00 ± 0.631	796	33.96 ± 0.854	<0.001	5	28.52 ± 3.864	0.253
HOMA-IR	363	1.86 ± 0.066	643	4.01 ± 0.126	<0.001		NA	
HbA1c	371	5.58 ± 0.025	794	8.49 ± 0.083	<0.001		NA	
Fasting Blood Sugar (mg/dl)	376	85.11 ± 0.414	796	155.84 ± 2.582	<0.001		NA	
Post Glucose Blood Sugar (mg/dl)	375	99.25 ± 1.057	795	260.85 ± 3.948	<0.001		NA	
FBS Insulin	362	8.84 ± 0.301	643	10.90 ± 0.282	<0.001		NA	
PGBS Insulin	341	56.98 ± 2.403	629	58.14 ± 1.879	0.996		NA	

* Clinical parameters of the overall Chennai population (n=3200) stratified as controls, DM/HTN cases and CAD cases were analysed.

Values are shown as mean ± SE. LVIDd: Left ventricular internal diameter at end of diastole, LVIDs: Left ventricular internal diameter at end of systole, HOMA-IR index: Insulin resistance index (Fasting insulin (mIU/L) x Fasting glucose (mg/dL)/405), HbA1c: glycated haemoglobin, FBS: fasting blood sugar, PGBS: post-glucose blood sugar. NA: Data not available.

Supplementary Table S3: Clinical characteristics of controls and cases in a North Indian population.*

Parameter	Controls		HTN cases		p value
	N	Mean \pm SE	N	Mean \pm SE	
Age (years)	358	59.77 \pm 0.619	377	47.45 \pm 0.619	<0.001
Sex (M/F)	358	71.2%/28.8%	377	51.2%/48.8%	
Systolic Blood Pressure (mm Hg)	359	118.48 \pm 0.589	388	149.43 \pm 0.787	<0.001
Diastolic Blood Pressure (mm Hg)	359	75.69 \pm 0.322	388	97.01 \pm 0.456	<0.001
Mean Arterial Pressure (mm Hg)	359	89.89 \pm 0.312	388	114.49 \pm 0.489	<0.001
Total Cholesterol (mg/dl)		NA	349	192.78 \pm 2.503	
Triglycerides (mg/dl)		NA	347	173.67 \pm 23.719	
High Density Lipoproteins (mg/dl)		NA	339	46.67 \pm 0.553	
Low Density Lipoproteins (mg/dl)		NA	344	128.51 \pm 1.934	

* Clinical parameters of the overall Chandigarh population (n=760) stratified as HTN cases and controls were analysed. Values are shown as mean \pm SE. NA: Data not available.

Supplementary Table S4: Distribution of genotypes and minor allelic frequencies in Indian populations.*

Genotypes	Chennai population		Chandigarh population	
	Cases	Controls	Cases	Controls
GG	1947 (87.5%)	868 (88.9%)	362 (90.3%)	345 (96.1%)
AG	264 (11.9%)	100 (10.2%)	39 (9.7%)	14 (3.9%)
AA	13 (0.6%)	8 (0.8%)	0 (0%)	0 (0%)
Total	2224 (100%)	976 (100%)	401 (100%)	359 (100%)
Minor Allelic Frequency (%)	6.34		3.48	

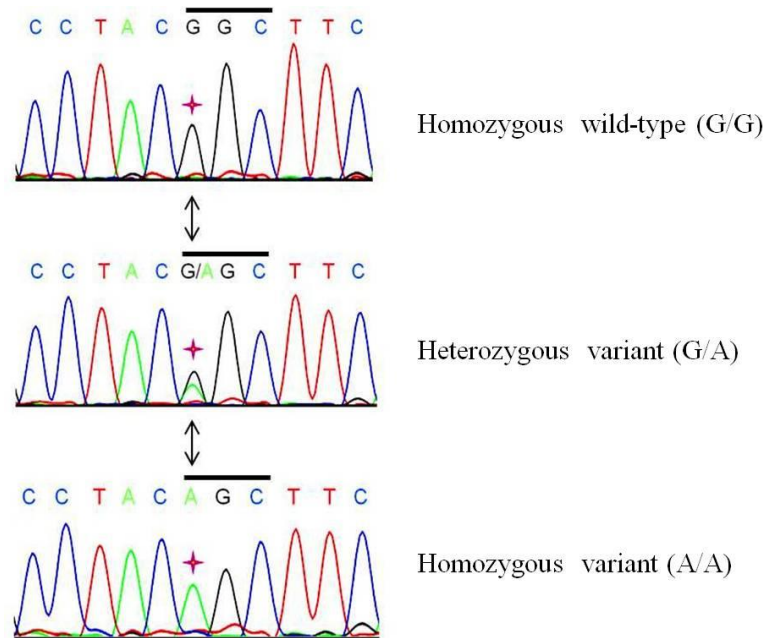
* The minor allelic frequencies were calculated for the Chennai DM (type-2 diabetes), HTN (hypertension) cases and controls, Chennai CAD (coronary artery disease) cases and Chandigarh HTN cases and controls. There was a drastic difference in the frequencies between the Chennai and Chandigarh populations ($\chi^2=18.01$ and $p=0.0001$).

Supplementary Table S5: Distribution of genotypes of Gly364Ser SNP in various ethnic/geographical world populations.*

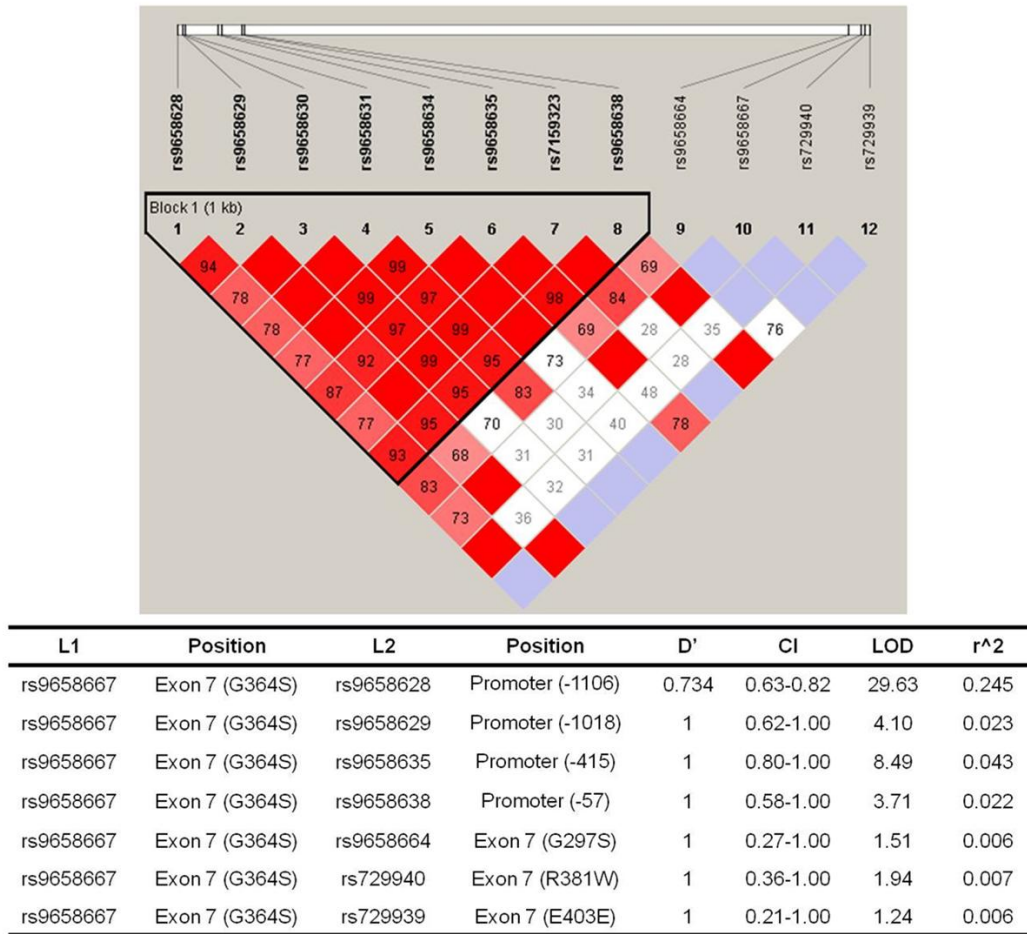
	Population	n	MAF (%)	Reference/Source
	Chinese (Metropolitan Denver, Colorado, USA)	82	7.3	dbSNP / Hapmap Data
	Gujarati Indian (Houston, Texas, USA)	87	6.9	dbSNP / Hapmap Data
Asian	Indian (Chennai, India)	3200	6.3	This study
	Japanese (Ibaraki, Saitama and Shizuoka, Japan)	343	6.1	Choi <i>et. al.</i> 2015 ²¹
	Indian (Chandigarh, India)	760	3.8	This study
	Asian (Southern California, USA)	44	1.8	dbSNP / Wen <i>et. al.</i> 2004 ²⁰
Hispanic	Hispanic (Southern California, USA)	28	5.9	dbSNP / Wen <i>et. al.</i> 2004 ²⁰
European	European (Southern California, USA)	52	4.9	dbSNP / Wen <i>et. al.</i> 2004 ²⁰
	European (ClinSeq Project)	230	2.4	dbSNP / Biesecker <i>et. al.</i> 2009 ²²
	Toscan (Italy)	84	2.4	dbSNP / Hapmap Data
African	Luhya (Webuya, Kenya)	87	1.1	dbSNP / Hapmap Data
	Maasai (Kinyawa, Kenya)	142	0.4	dbSNP / Hapmap Data
	African (Southern California, USA)	57	0.0	dbSNP / Wen <i>et. al.</i> 2004 ²⁰

*The minor allele frequencies for the Gly364Ser variant in various populations of the world are listed. While the Chennai populations showed minor allele frequencies similar to other Asian populations, the Chandigarh population showed a frequency closer to that displayed by European populations.

SUPPLEMENTARY FIGURES



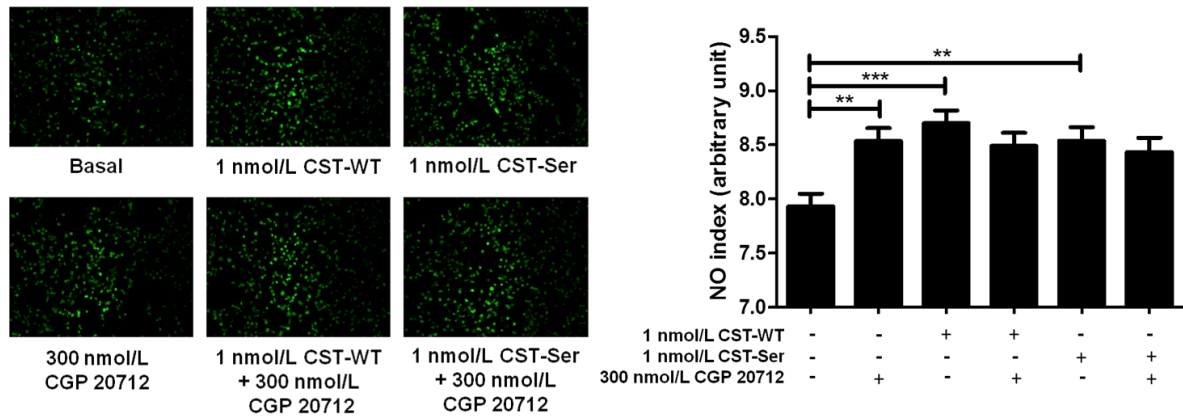
Supplementary Figure S1. Discovery of the naturally-occurring amino acid variant Gly364Ser of catestatin. Resequencing of the catestatin region of the chromogranin A gene was carried out using specific primers. Representative chromatograms for wild-type GG (Gly/Gly), heterozygous variant GA (Gly/Ser) and homozygous variant AA (Ser/Ser) at 9559 bp position are shown. The amino acid number indicated, i.e., 364, is with respect to the mature chromogranin A protein, which is equivalent to the 382nd amino acid in the pre-protein that includes the 18 aa long signal peptide. Here, the 1st nucleotide (indicated by *) of the codon GGC (in the wild-type) is altered to AGC (in the variant) changing the amino acid Gly to Ser.



Supplementary Figure S2. Linkage disequilibrium (LD) among CST Gly364Ser and other *CHGA* variants.

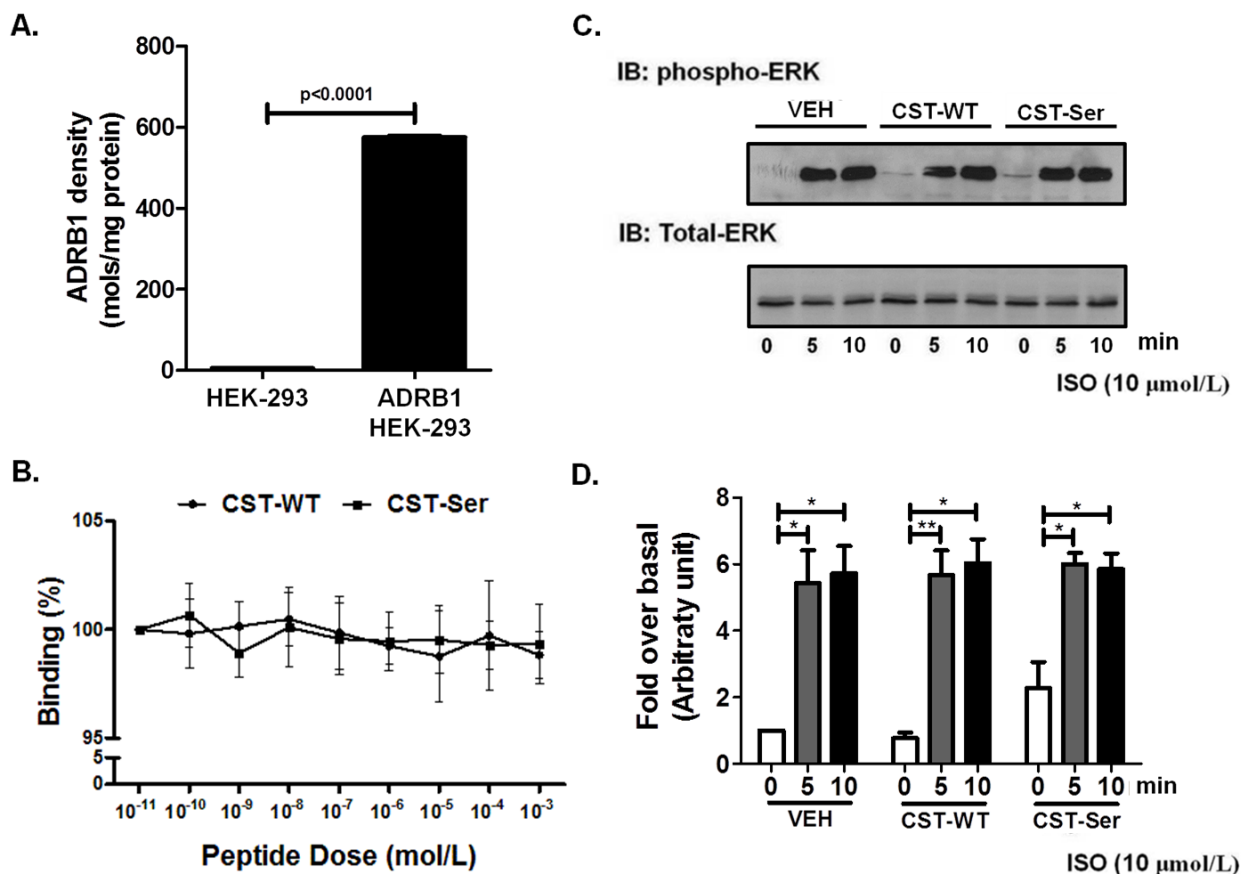
LD pattern of 12 common biallelic polymorphisms discovered in the *CHGA* promoter and exon-7 region of 581 individuals. Pairwise results are plotted on a pseudocolor scale for LD with Haploview. Bright red represents $D'=1, LOD \geq 2$; blue represents $D'=1, LOD < 2$; shades of pink/red represent $D' < 1, LOD \geq 2$; white represents $D' < 1, LOD < 2$. Number in diamond shape represents LD as $D' \times 100$. LD blocks are determined by the four-gamete rule.

LOD: logarithm of odds.



Supplementary Figure S3. Effect of ADRB1 antagonist CGP 20712 on NO production in HUVECs treated with CST peptides.

The fluorescence intensities (NO indices) were calculated by Image J analysis and plotted as mean \pm SE. The experimental groups were compared by one-way ANOVA followed by Tukey's multiple comparison post-test. Representative images for the treatment of HUVECs with 300 nmol/L CGP 20712, 1 nmol/L CST-WT, 1 nmol/L CST-364Ser, 1 nmol/L CST-WT + 300 nmol/L CGP 20712, 1 nmol/L CST-364Ser + 300 nmol/L CGP 20712. *** represents $p < 0.001$ for basal vs. CST-WT peptide, ** represents $p < 0.01$ for basal vs. CGP 20712, basal vs. CST-364Ser. Overall one-way ANOVA $F=4.727$, $p=0.0003$; $n=450$ cells/condition.



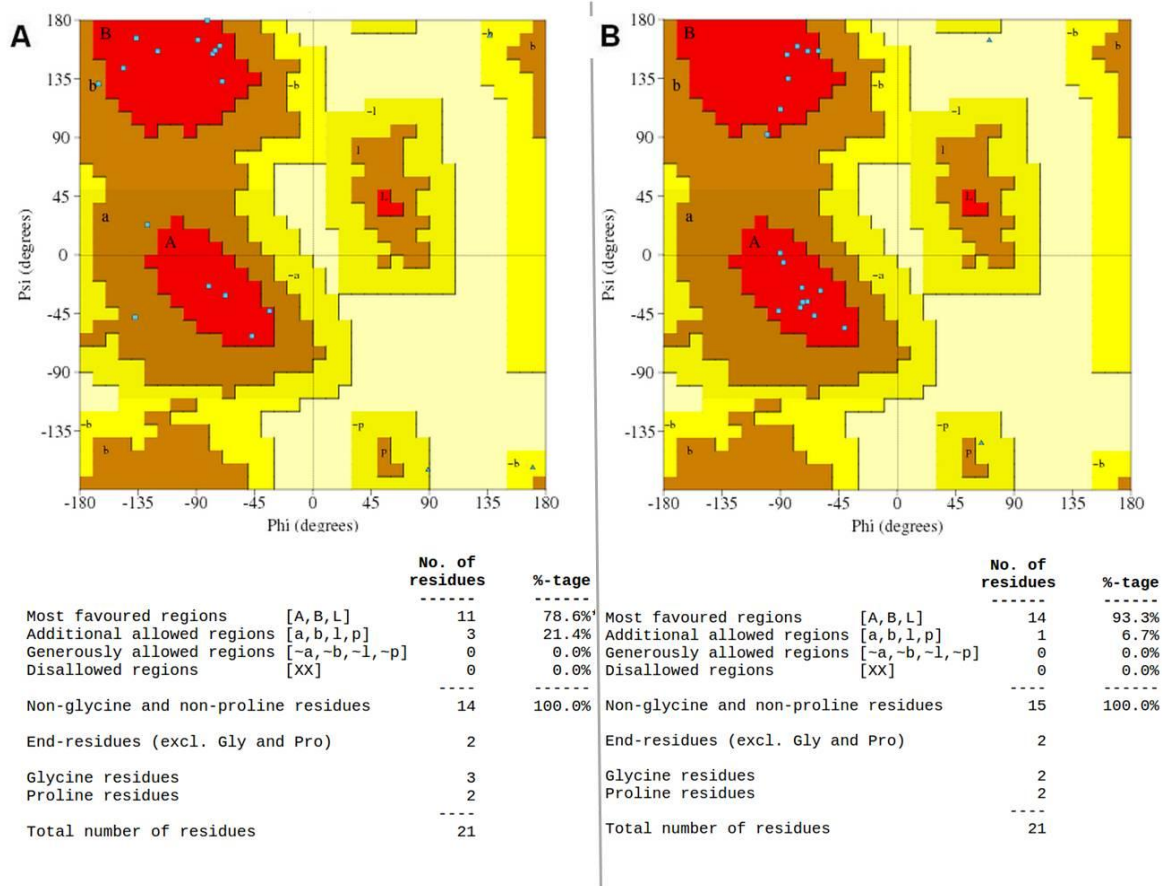
Supplementary Figure S4. Binding of CST peptides to ADRB1 receptor and downstream effects.

Panel A: ADRB1 HEK-293 cells showed ~109-fold higher expression of ADRB1 ($p < 0.0001$) as compared to control HEK-293 cells. Data are shown as ADRB1 levels normalized with total protein.

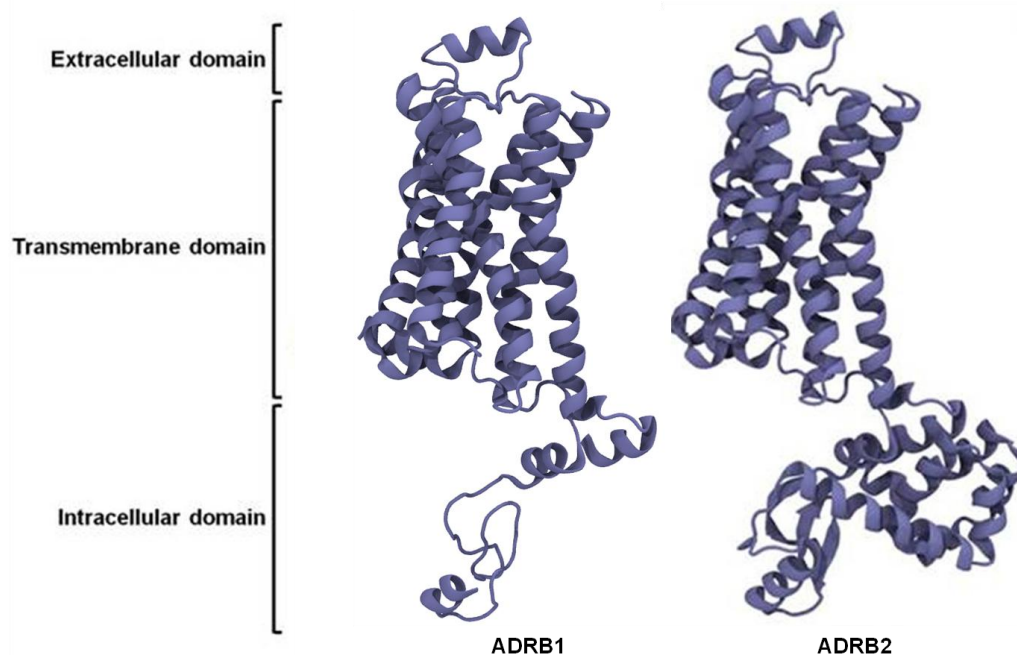
Panel B: Data are shown as percentage binding of the radio-ligand cyanopindolol. With increasing doses of CST-WT and CST-364Ser (10 pmol/L to 1 mmol/L), there was no displacement of the ligand. The experimental groups were compared by one-way ANOVA followed by Tukey's multiple comparison post-test.

Panels C and D: Representative western blot (panel C) and quantitative representation of the densitometric analysis from 4 independent experiments (panel D) showing phosphorylated ERK (pERK) and total ERK levels upon treatment with CST peptides and isoproterenol

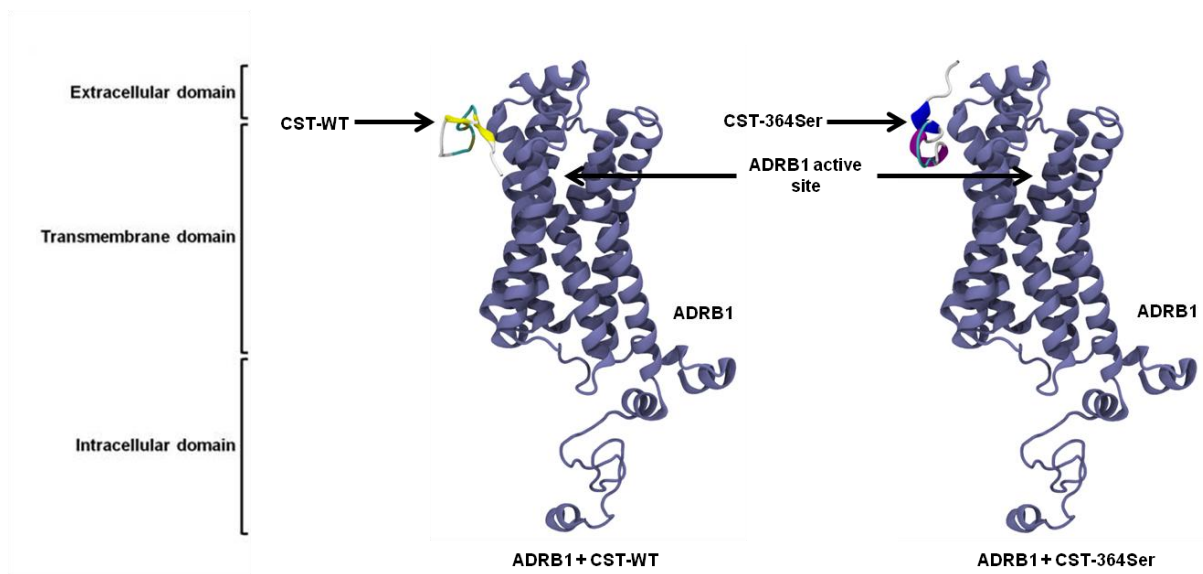
(ISO). ISO (10 $\mu\text{mol/L}$) showed an increase in pERK levels at 5 min and 10 min in the vehicle (VEH) condition, reflecting the activation of ADRB1. However, this increase remain unaffected upon pre-treatment with both CST-WT (10 $\mu\text{mol/L}$) and CST-364Ser (10 $\mu\text{mol/L}$). The experimental groups were compared by t-test.



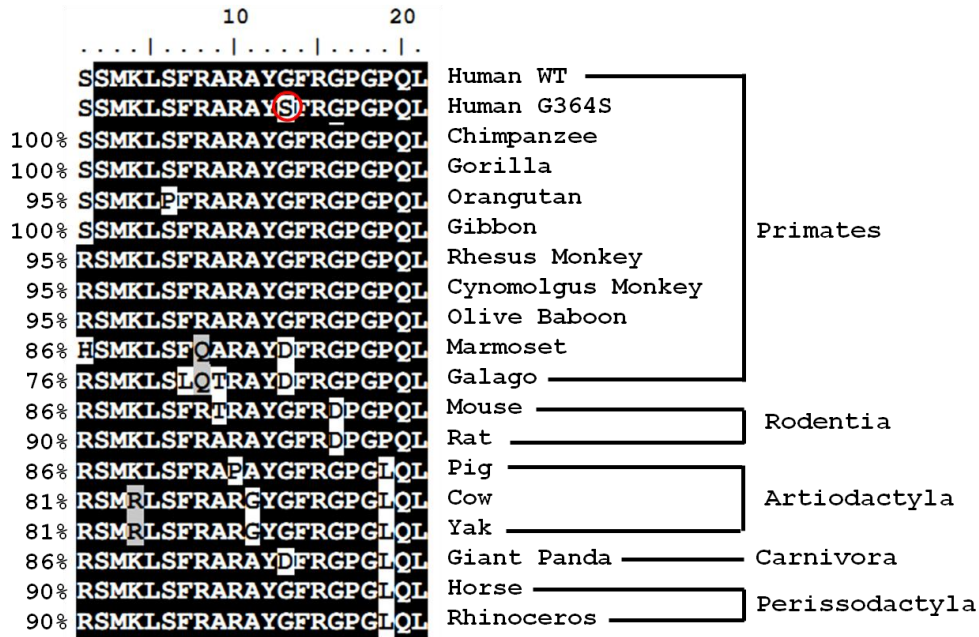
Supplementary Figure S5. Ramachandran plots for the modelled structures of CST-WT and CST-364Ser peptides. Panel A and Panel B are the Ramachandran plots for CST-WT and CST-364Ser, respectively. In both the panels, the yellow, brown and red colored areas represent generously allowed, additionally allowed and most favoured regions, respectively. Amino acid residues falling in the allowed region are represented by blue dots. Regions A, B and L correspond to the residues involved in the formation of right handed alpha-helices, beta-sheets and left handed alpha-helices, respectively.



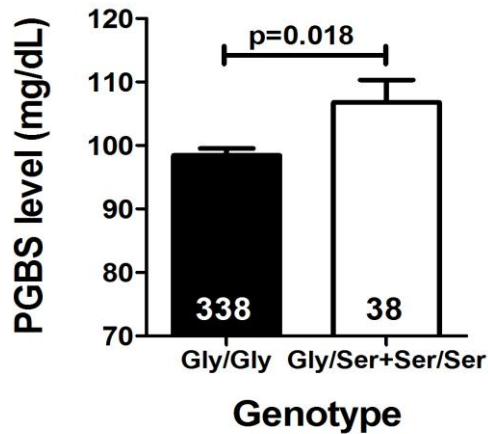
Supplementary Figure S6. Modelled structure of human beta1- and beta2-adrenergic receptor (ADRB1/2). The figure shows the 3-dimensional conformation of ADRB1 (left) and ADRB2 (right) in cartoon representation. The structure of ADRB2 is based on the crystal structure of ADRB2 with resolution 2.4 Å obtained from protein data bank (PDB ID:2RH1). The bound ligands and the crystal water were stripped from the protein crystal structure and subsequently energy minimized to obtain the above sophisticated model of ADRB2 for protein-protein docking. The structure of ADRB1 was modelled based on the template of ADRB2. The extracellular domain, the transmembrane domain and the intracellular domain have been labelled.



Supplementary Figure S7. Interactions of CST peptides with ADRB1. The figure shows the docking of CST-WT (left) and CST-364Ser (right) to ADRB1. ADRB1 is colored violet, the beta-sheet in CST-WT is shown in yellow, while the alpha-helix and 3_{10} -helix in CST-364Ser are shown in purple and blue respectively.



Supplementary Figure S8. Human CST variants and inter-species homology among Eutherian mammals. ClustalW multiple sequences alignment was carried out using BioEdit version 7.2.5 (Ibis Biosciences, Carlsbad, CA, USA); the percentages of homology are given on the left side. These organisms are arranged according to their Order. Human variant is encircled in red. The identical amino acid residues from all species are shaded with dark grey color and similar amino acid residues are shaded with light grey color. All the species showed a minimum of 76% similarity in CST region of *CHGA*. CST sequences used are - Primates: Human (accession number NM_001275), Common chimpanzee (XP_510135.3), Gorilla (XP_004055643.1), Sumatran orang-utan (XP_002825091.1), White-cheeked gibbon (XP_003260951.1), Rhesus monkey (XP_001092629.2), Cynomolgus monkey (BAE01874.1), Olive baboon (XP_003902238.1), Marmoset (XP_002754260.1) and Galago (XP_003787045.1), Rodentia: House mouse (NP_031719.1) and Common rat (AEB41037.1), Artiodactyla: Wild pig (NP_001157477.2), Cow (NP_851348.1) and Yak (ELR47684.1), Carnivora: Giant panda (XP_002923879.1), Perissodactyla: Horse (NP_001075283.1) and White rhinoceros (XP_004434274.1)



Supplementary Figure S9. Allele-specific associations of human post-glucose blood sugar levels *in vivo*. In the Chennai controls population, subjects were stratified into Gly/Gly and Gly/Ser+Ser/Ser groups. The post-glucose blood sugar levels, measured by standard biochemical assays, were compared between the two groups. Data are shown as mean \pm SE. Statistical significance between the groups was determined by Levene's test for equality of variances and t-test for equality of means using SPSS software (SPSS Inc., Chicago, IL). The PGBS levels in 364Ser carrying individuals were elevated than wild-type individuals in this population.